Discharge Flow-Photoionization Mass Spectrometric Study of HNO: Photoionization Efficiency Spectrum and Ionization Energy and Proton Affinity of NO

Szu-Cherng Kuo,[†] Zhengyu Zhang,[‡] Stuart K. Ross,[§] and R. Bruce Klemm*,[||]

Brookhaven National Laboratory, Building 815, P.O. Box 5000, Upton, New York 11973-5000

Russell D. Johnson, III[⊥]

Physical and Chemical Properties Division, National Institute of Standards and Technology, Gaithersburg, Maryland 20899

Paul S. Monks,[▽] R. Peyton Thorn, Jr.,[#] and Louis J. Stief*,[¶]

Laboratory for Extraterrestrial Physics (Code 690), NASA/Goddard Space Flight Center, Greenbelt, Maryland 20771

Received: February 17, 1997; In Final Form: April 8, 1997[⊗]

Photoionization efficiency (PIE) spectra of HNO were measured over the wavelength range $\lambda = 110-125$ nm and in the ionization threshold region, $\lambda = 118-124$ nm, using a discharge flow-photoionization mass spectrometer (DF-PIMS) apparatus coupled to a synchrotron radiation source. HNO was generated *in situ* by the following reaction sequence: $N + NO \rightarrow N_2 + O$; $O + C_2H_4 \rightarrow CH_3 + HCO$; $HCO + NO \rightarrow HNO + CO$. The PIE spectrum displays steplike behavior near threshold and an HN−O stretching frequency in the cation of 1972 ± 67 cm^{-1}. A value of $10.18_4 \pm 0.01_2$ eV for the adiabatic ionization energy (IE) of HNO was obtained from photoionization thresholds, which correspond to the $HNO^+(X^2A') \leftarrow HNO(X^1A')$ transition. This result is the first PIMS determination of IE(HNO). Also, an *ab initio* molecular orbital calculation (QCISD(T)/aug-cc-pVQZ) was performed that yields a value for IE(HNO) of 10.186 ± 0.050 eV. There is good agreement between the experimental and the theoretical values for IE(HNO) reported here and that from a recent photoelectron spectroscopy study. The present experimental value for IE(HNO) was employed along with other, known thermodynamic quantities to obtain values for the heat of formation of the HNO cation and the absolute proton affinity of NO: $\Delta_f H°_{298}(HNO^+) = 1089.73 \pm 1.18$ kJ mol^{-1} ($\Delta_f H°_0(HNO^+) = 1092.65 \pm 1.18$ kJ mol^{-1}); $PA_{298}(NO) = 531.55 \pm 1.26$ kJ mol^{-1} ($PA_0(NO) = 526.12 \pm 1.26$ kJ mol^{-1}).

Introduction

Nitrosyl hydride, HNO, is an important intermediate in combustion,[1,2] and it has been detected in the interstellar medium.[3,4] The association of hydrogen atoms with nitric oxide to form HNO

$$NO + H + M \rightarrow HNO + M$$
$$k_1 = 1.5 \times 10^{-32} \exp(300/T) \text{ cm}^6 \text{ molecule}^{-2} \text{ s}^{-1} \quad (M = H_2, \text{ ref 1}) \quad (1)$$

is similar to the reaction of hydrogen atoms with O_2 to give HO_2. Subsequent reaction of HNO with hydrogen atoms

$$HNO + H \rightarrow H_2 + NO$$
$$k_2(298 \text{ K}) = 5.6 \times 10^{-12} \text{ cm}^3 \text{ molecule}^{-1} \text{ s}^{-1} \quad (\text{ref 2b}) \quad (2)$$

has been invoked to account for the catalytic effect of NO on the recombination of hydrogen atoms in discharge-flow systems[5,6] and in flames.[7,8] The species has also been implicated in the "thermal De-NO_x" process[9] and in the reduction of NO by H_2.[10,11] In interstellar clouds, formation of HNO probably occurs *via* both gas phase and grain-surface chemistry,[3b] while it is destroyed in the gas phase *via* reaction 2. Studies of the interstellar abundance of HNO are of interest because there are few detected species that contain the N−O bond.

Four years after Smallwood[5] suggested the existence of HNO, Harteck[12] reported collecting, at liquid nitrogen temperatures from a discharge-flow system, an explosive solid that had the empirical formula HNO. However, it was not until 25 years later that HNO was finally observed in the gas phase *via* absorption spectroscopy by Dalby.[13] The species has been detected by mass spectrometry,[14−17] and its emission and absorption spectra have been investigated by several groups.[18−21] Thermodynamic properties of HNO[22,23] and HNO^+ (refs 24−27) have been compiled and evaluated. There have also been numerous theoretical studies of HNO/NOH and HNO^+/NOH^+ to determine thermochemical properties, barriers to isomerization, and potential energy surfaces.[28−34]

Despite the extensive investigation of HNO, there are few reported studies of direct ionization of this species. Kohout

* Authors to whom correspondence should be sent.
[†] Present address: TRW Electronics Systems & Technology Division, Redondo Beach, CA 90278. Email: kuo@bnl.gov.
[‡] Present address: Philips Lighting, Nanjing, People's Republic of China.
[§] Visiting Research Associate, Department of Chemistry, University of Aberdeen, Meston Walk, Aberdeen AB9 2UE, Scotland, U.K. Present address: Protection and Decontamination Department, CBD Porton Down, Salisbury, Wiltshire SP4 0JQ, U.K.
[||] Email: klemm@sun2.bnl.gov.
[⊥] Email: rdj3@enh.nist.gov.
[▽] NAS/NRC Resident Research Associate. Present address: Chemistry Department, University of Leicester, University Road, Leicester LE1 7RH, England. Email: psm7@le.ac.uk.
[#] NAS/NRC Resident Research Associate. Email: ysrpt@lepvax.gsfc.nasa.gov.
[¶] Email: ulljs@lepvax.gsfc.nasa.gov.
[⊗] Abstract published in *Advance ACS Abstracts,* May 15, 1997.

S1089-5639(97)00594-X CCC: $14.00

and Lampe[14] appear to have reported the first measurement for the ionization energy (IE) of HNO. They employed electron impact mass spectrometry (EIMS) to determine a value of 10.29 ± 0.14 eV for the IE of $D^{15}NO$.[14b] By using *ab initio* calculations to determine differences in zero-point energies, Bruna and Marian[31b] corrected Kohout and Lampe's value to obtain IE(HNO) = 10.23 eV. Calculated values for IE(HNO) have been reported by Chong et al.[28] (vertical IE = 10.66 eV) and Bruna[31c] (vertical IE = 10.05 eV, adiabatic IE = 9.75 eV). The IE of HNO has also been determined *via* photoelectron spectroscopy (PES). In a preliminary PES study at low resolution, a value of 10.1 ± 0.1 eV[17a] was obtained, while a more precise value, 10.18 ± 0.01 eV, was reported by Baker et al.,[17b] who employed a single-detector photoelectron spectrometer. However, in the PES study of Baker et al.,[17b] the HNO spectrum was severely perturbed by overlapping structure due to NO, HNOH, and NH_2OH. It is interesting to note that, for whatever reason, no value for IE(HNO) was recommended in the latest NIST positive ion database.[27] Also, it is important to mention that Levin and Lias[24] incorrectly attribute a value for the vertical IE of HNO to Rao (*Indian J. Chem.* **1975**, *13*, 950). Actually, the species referred to was CH_3NO, not HNO.

In this study, we present the first determination of the HNO photoionization efficiency (PIE) spectrum and the photoionization threshold from which the ionization energy may be determined. This result is compared with previous experimental values and with a theoretical value obtained in this work from *ab initio* molecular orbital calculations. By using IE(HNO) and other available thermodynamic quantities, the heat of formation of HNO^+ and the absolute proton affinity (PA) of NO were also computed.

Experimental Section

Experiments were performed by employing a discharge flow-photoionization mass spectrometer (DF-PIMS) apparatus coupled to beam line U11 at the National Synchrotron Light Source (NSLS) at Brookhaven National Laboratory. The apparatus and experimental procedures have been described in detail in previous publications.[35−40]

Reaction 1 is too slow to contribute to the generation of HNO under our experimental conditions, since $k_1(298\ \mathrm{K}) \approx 6 \times 10^{-15}$ $\mathrm{cm^3\ molecule^{-1}\ s^{-1}}$ at a pressure of 4 Torr in He. In this study, HNO was produced in a Teflon-lined flow reactor by the reaction sequence

$$N + NO \rightarrow N_2 + O(^3P)$$
$$k_3(298\ \mathrm{K}) = 3.0 \times 10^{-11}\ \mathrm{cm^3\ molecule^{-1}\ s^{-1}} \quad \text{(ref 41)} \quad (3)$$

$$O(^3P) + C_2H_4 \rightarrow HCO + CH_3$$
$$k_4(298\ \mathrm{K}) = 7.29 \times 10^{-13}\ \mathrm{cm^3\ molecule^{-1}\ s^{-1}} \quad \text{(ref 42)} \quad (4)$$

$$HCO + NO \rightarrow HNO + CO$$
$$k_5(298\ \mathrm{K}) = 1.20 \times 10^{-11}\ \mathrm{cm^3\ molecule^{-1}\ s^{-1}} \quad \text{(ref 43)} \quad (5)$$

Nitrogen atoms were generated by passing a N_2/He mixture through a microwave discharge (<70 W, 2450 MHz) at the upstream end of the flow tube (about 100 cm from the nozzle). Excited N and N_2 from the discharge were quenched in a recombination volume before the N atoms entered the upstream end of the flow tube. N-atom concentrations were determined by using NO titration (i.e., reaction 3). In some early measurements, a NO/C_2H_4/He mixture was introduced through the tip of the movable injector at a distance of 10−15 cm from the sampling nozzle to allow for a reaction time of about 10 ms. For most of the measurements, the NO/He mixture was introduced near the upstream end of the flow tube to facilitate reaction with N atoms, and the C_2H_4/He mixture was introduced through the tip of the movable injector at a distance of 5−10 cm from the sampling nozzle. The optimized yield of HNO was achieved with this second approach. Potential secondary reactions such as N + C_2H_4 (early approach) and $O(^3P)$ + NO + He (in both approaches) are too slow to be significant under our conditions. All experiments were conducted at ambient temperature ($T = 298 \pm 2$ K) and at a flow reactor pressure of about 4.1 ± 0.2 Torr with helium carrier gas. Flow velocities were in the range of 1400−1590 cm s^{-1}. The concentrations of C_2H_4, N_2, and NO in the flow reactor were, in units of molecules cm^{-3}, (2.5−16) × 10^{14}, (0.9−49) × 10^{14}, and (0.5−6.9) × 10^{14}, respectively.

The gaseous mixture in the flow reactor was sampled as a molecular beam into the sample chamber and subsequently into the photoionization source of the mass spectrometer. Ions were mass selected with an axially aligned quadrupole mass filter, detected with a channeltron/pulse preamplifier, and thence counted for preset integration times. Measurements of PIE spectra, the ratio of ion counts/light intensity versus wavelength, were made using tunable vacuum-ultraviolet (VUV) radiation at the NSLS as the ionization source. A monochromator with a normal incidence grating (1200 lines/mm) was used to disperse the VUV light,[40] and a LiF window ($\lambda \geq 104$ nm) was used to eliminate second- and higher-order radiation. The intensity of the VUV light was monitored *via* a sodium salicylate coated window with an attached photomultiplier tube.

The nitrogen, helium, and ethylene were of the highest purity obtainable (MG Industries, scientific grade, 99.9995%, 99.9999%, and 99.95%, respectively) and were used directly from cylinders. The nitric oxide (MG Industries, C. P. grade, 99.0%) was purified by thorough outgassing at 77 K followed by vacuum distillation from 91 to 77 K.

Results and Discussion

As an example of the PIMS experiment, the PIE spectrum of NO, from the photoionization reaction $NO(X^2\Pi) + h\nu \rightarrow NO^+(X^1\Sigma^+)$, was measured over the wavelength range of λ = 120−136 nm at a nominal resolution of 0.16 nm (fwhm) and at 0.1 nm intervals. As shown in Figure 1, the onset of ionization at λ = 133.85 nm, taken as the half-rise point of the first step, corresponds to an adiabatic ionization energy of 9.263 ± 0.011 eV. This result is in good agreement with the recommended value of 9.26405 ± 0.00006 eV,[27] and it demonstrates that the wavelength calibration, established by the location of zero order, is excellent.[38,39] In addition, to the onset, the PIE spectrum of NO displays autoionizing structure superposed upon a steplike vibrational progression. The first four vibrational levels in the cation are shown in the spectrum.

A. Determination of IE(HNO). A mass scan (at λ = 110 nm) of the reactant, NO (m/z = 30), is shown in Figure 2a. The trace amount of signal at m/z = 31 is from the natural abundances of ^{15}N and ^{17}O isotopes (0.37% and 0.038%, respectively).[44] Figure 2b shows the mass scan (at λ = 110 nm) when the microwave discharge of N_2 is turned on (see Experimental Section). The increase of the signal at m/z = 31 is due to the generation of HNO.

Modeling reactions 3−5 under the optimized yield condition (see Experimental Section) using the CHEMKIN code[45] shows that this reaction sequence is essentially complete within 3.5

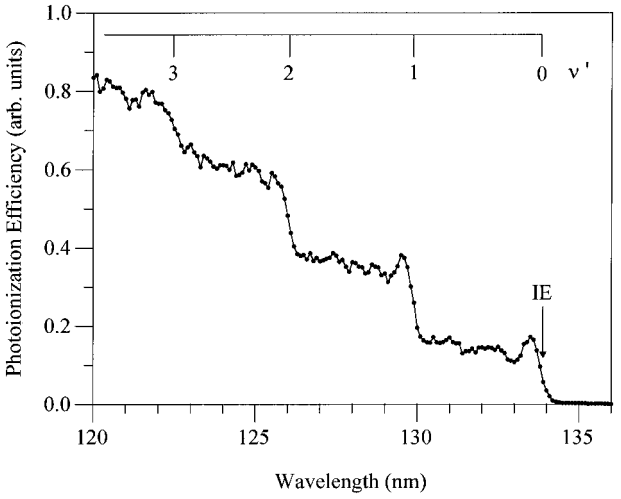

Figure 1. Photoionization efficiency spectrum of NO between λ = 120.0 and 136.0 nm at a nominal resolution of 0.16 nm and 0.1 nm steps. The photoionization efficiency is ion counts at $m/z = 30$ divided by the light intensity in arbitrary units. The onset of ionization, at λ = 133.85 nm, yields IE = 9.263 ± 0.011 eV where the uncertainty is conservatively estimated from the wavelength resolution, 0.16 nm. [NO] = 9.5×10^{13} molecules cm^{-3}. The positions of the "steps" in the PIE curves (122.45, 126.05, 129.85, and 133.85 nm) are indicated by the superposed lines.

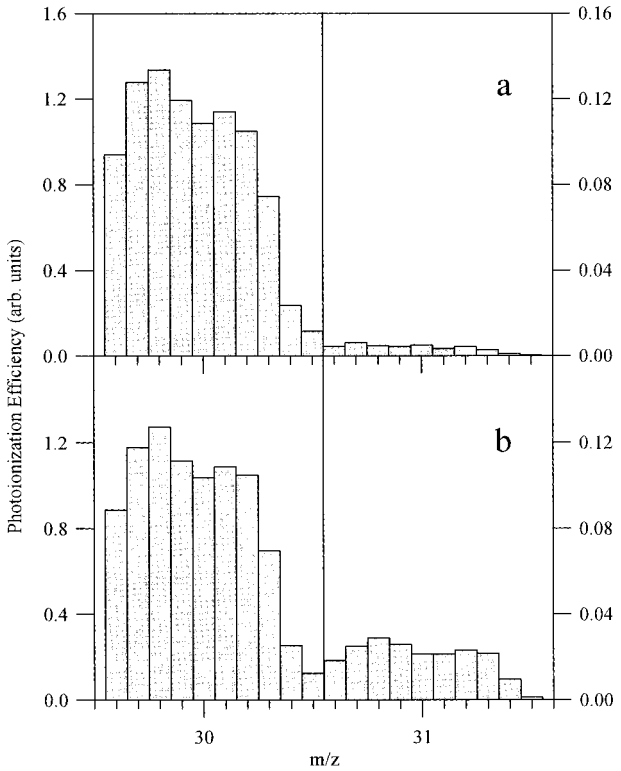

Figure 2. Mass scans over the range of m/z = 29.6−31.5 at m/z = 0.1 steps and at an excitation wavelength of 110 nm (11.27 eV). Note that there are different scales for $m/z = 30$ and $m/z = 31$. (a) With the microwave discharge OFF, the peak at $m/z = 31$ is due to the isotopes ^{15}NO and N^{17}O. (b) With the microwave discharge ON, the peak at $m/z = 31$ is due to HNO as well as the isotopes ^{15}NO and N^{17}O. $[NO]_0 = 5.1 \times 10^{13}$ molecules cm^{-3}, $[C_2H_4]_0 = 2.5 \times 10^{14}$ molecules cm^{-3}, and $[N_2]_0 = 8.8 \times 10^{13}$ molecules cm^{-3}.

ms (i.e., the reaction time with the injector at a distance of 5 cm from the sampling nozzle), and the maximum HNO concentration is about 1.2×10^{13} molecules cm^{-3}. However, for $[N]_0 \approx 1.2 \times 10^{13}$ atoms cm^{-3} and $[NO]_0 = 3.3 \times 10^{14}$ molecules cm^{-3}, the sum of the concentrations of ^{15}NO and

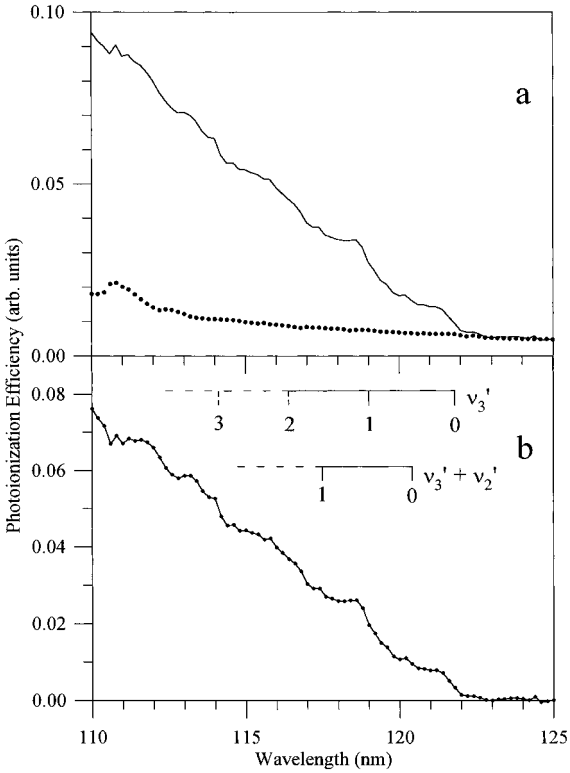

Figure 3. Photoionization efficiency spectra of HNO between λ = 110 and 125 nm at a nominal resolution of 0.16 nm and 0.2 nm steps. (a) The solid line is the PIE signal at $m/z = 31$, presumably from HNO as well as the isotopes ^{15}NO and N^{17}O. The filled circles are the residual signal from NO isotopes. (b) The PIE spectrum for HNO, after correcting the residual signal from NO isotopes. The main vibrational progression ($\nu_3' = 0-3$) has "steps" at 121.8, 119.0, 116.4, and 114.1 nm, respectively. The minor progression ($\nu_3' + \nu_2'$) has "steps" at 120.4 and 117.5 nm. $[NO]_0 = 3.3 \times 10^{14}$ molecules cm^{-3}, $[C_2H_4]_0 = 1.6 \times 10^{15}$ molecules cm^{-3}, and $[N_2]_0 = 4.8 \times 10^{15}$ molecules cm^{-3}.

N^{17}O (0.408% of normal NO)[44] is calculated to be about 1.2×10^{12} molecules cm^{-3} (taking into account the loss of NO due to reactions 3 and 5), and therefore it was necessary to perform a correction to the $m/z = 31$ signal for these isotopic contributions.

The PIE spectrum for HNO, generated *via* reactions 3−5, is shown in Figure 3 over the wavelength range of λ = 110−125 nm at 0.16 nm resolution and at 0.2 nm intervals. The solid line in Figure 3a is the PIE signal at $m/z = 31$, presumably due to the contribution of HNO as well as the isotopes ^{15}NO and N^{17}O. The filled circles in Figure 3a represent the residual signal from the NO isotopes, as determined in a separate experiment. After the residual NO signal was corrected for, the PIE spectrum for HNO was obtained, as shown in Figure 3b. This spectrum displays vibrational steps ($\nu_3' = 0-3$) in the cation, corresponding to the HN−O stretch mode in the cation. From the first two steps in the main progression (Figure 3b), a value of 1932 cm^{-1} is obtained for the vibrational spacing. Similarly, the minor progression ($\nu_3' + \nu_2'$) yields a value of 2050 cm^{-1} for ν_3', and from the difference between the two progressions we obtain a value of 955 cm^{-1} for the bend frequency (ν_2').

In order to better determine the ionization energy, detailed examinations near the threshold were carried out, and an example is plotted in Figure 4. The spectrum for HNO was obtained (Figure 4) in the wavelength region λ = 118−124 nm at 0.1 nm intervals and a nominal resolution of 0.16 nm (fwhm). This spectrum was corrected for the effects of the NO isotopes, as discussed above. The threshold (see Figure 4) was analyzed

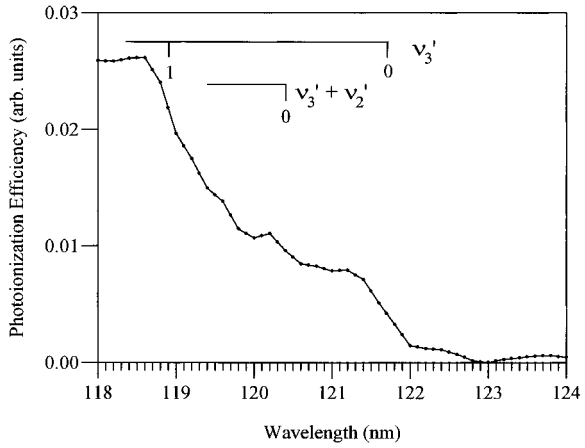

Figure 4. Photoionization threshold region of HNO at a nominal resolution of 0.16 nm and 0.1 nm steps between $\lambda = 118$ and 124 nm. The onset of ionization is at $\lambda = 121.70$ nm (10.188 ± 0.013 eV). The main vibrational progression ($\nu_3' = 0$ and 1) displays "steps" at 121.7 and 118.9 nm. The minor progression ($\nu_3' + \nu_2'$) has a weak step at 120.4 nm. The data in this figure are a summation from four individual spectra with $[NO]_0$, $[C_2H_4]_0$, and $[N_2]_0$ similar to the levels used in the run shown in Figure 3.

TABLE 1: Threshold Wavelengths and Ionization Energies for HNO

threshold (nm)	IE (eV)	nominal λ step (nm)	fwhm (nm)
121.85	10.175 ± 0.019	0.1	0.23
121.60	10.196 ± 0.019	0.1	0.23
121.75	10.184 ± 0.013	0.1	0.16
121.80	10.179 ± 0.013	0.1	0.16
121.70	10.188 ± 0.013	0.1	0.16
121.7	$10.18_8 \pm 0.01_3$	0.2	0.16
121.7	$10.18_8 \pm 0.01_2$	0.2	0.14
121.7	$10.18_8 \pm 0.01_9$	0.2	0.23
121.8	$10.17_9 \pm 0.01_3$	0.2	0.16
121.8	$10.17_9 \pm 0.01_3$	0.2	0.16
121.7	$10.18_8 \pm 0.01_3$	0.2	0.16
121.8	$10.17_9 \pm 0.01_3$	0.2	0.16
mean	$\langle 10.18_4 \pm 0.01_2 \rangle$ (2σ)		

by taking the half-rise point of the initial step to derive the ionization energy. From Figure 4, a threshold wavelength, $\lambda = 121.70$ nm, is obtained, and thus the IE is 10.188 eV, corresponding to the transition $HNO^+(X^2A') \leftarrow HNO(X^1A')$. Table 1 lists 12 independent determinations of IE(HNO) with an average value for IE(HNO) of $10.18_4 \pm 0.01_2$ eV (where the uncertainity is given at the 2σ level). This value of IE(HNO) agrees well with the PES result of 10.18 ± 0.01 eV reported by Baker et al.,[17b] and there is reasonable agreement with the low-resolution PES result (10.1 ± 0.1 eV)[17a] and the corrected EIMS value of Kohout and Lampe (10.23 ± 0.14 eV).[14b,31b]

In Figure 4, the vibrational spacing ($0 \leftarrow 0$ to $1 \leftarrow 0$), corresponding to the HN−O stretch (ν_3') mode in the cation, is 1935 ± 100 cm^{-1} (where the uncertainty is derived from the wavelength resolution, 0.16 nm). Also, from the indicated separation between the two progressions, we obtain a value of 887 cm^{-1} for the bend vibrational spacing in the cation. Combining the values from Figure 3b with those from Figure 4, we obtain 1972 ± 67 cm^{-1} for the stretch vibrational spacing and about 921 cm^{-1} for the bend vibrational spacing. These values are in good to reasonable agreement with those from the PES study reported by Baker et al.:[17b] 1960 ± 30 cm^{-1} for ν_3' and 1090 ± 40 cm^{-1} for ν_2'.

B. *Ab Initio* Molecular Orbital Calculation of IE(HNO). Since the present study represents the first PIMS determination of the ionization energy of HNO, our results will be compared with a theoretical IE(HNO) obtained from *ab initio* molecular orbital calculations. All calculations were performed using the GAUSSIAN 94 suite of programs[46] with the internally supplied basis sets. To obtain the ionization energy of HNO we calculated the energy for the following isogyric reaction:

$$HNO + H_2CO^+ \rightarrow HNO^+ + H_2CO \qquad (6)$$

Isogyric reactions allow for some cancellation of errors in calculating energy differences between states with different spins. The energy of the reaction is the difference between the ionization energies of HNO and H_2CO, i.e. $\Delta E_r = IE(HNO) - IE(H_2CO)$. Using the known value, $IE(H_2CO) = 10.874 \pm 0.002$ eV,[47] the ionization energy of HNO can be determined.

The geometries and harmonic vibrational frequencies were calculated at the QCISD/cc-pVTZ level. These are listed in Tables 2 and 3 along with experimental vibrational frequencies, where known. Other computational studies have addressed the ground state geometry and vibrations of the neutral[33c,48−50] and cation.[30,31b] We have calculated the geometry and vibrational frequencies for the four species of interest using a common level of theory. In order to compare the result with experimental ionization energy determinations, we need the vibrational zero-point energies. The true vibrational frequencies show appreciable anharmonicity for the NH and CH stretches. This is seen in the 2684 cm^{-1} NH symmetric stretch observed in HNO[51,52] and our calculated value of 2977.5 cm^{-1}. To obtain a better estimate of the zero-point energies, we have used the experimentally observed vibrational frequencies where known,[17b,33c,51−55] and scaled our calculated values in the absence of experimental vibrational data. The scale factors were determined by comparing the known experimental vibrational frequencies with our calculated frequencies. One scaling factor was used for the hydrogen stretches and another scaling factor for the other vibrations. For the unknown NH stretch in the HNO cation we used the NH stretch scaling factor determined for the neutral. For the H_2CO cation, the scaling factor for the unknown vibrations was determined from the experimentally known cation vibrations.

To refine the ionization energies further, we used a larger basis set and included triples in the quadratic configuration interaction: QCISD(T)/aug-cc-pVQZ. These energies are listed in Table 4. The ionization energy from the calculations is 10.186 ± 0.050 eV (2σ). The uncertainty is estimated from

TABLE 2: Geometries of HNO and H_2CO Calculated at the QCISD/cc-pVTZ Level

	HNO		H_2CO	
	neutral	cation	neutral	cation
r_H (Å)[a]	1.0528	1.0656	1.1017	1.1104
r_0 (Å)[b]	1.2051	1.1267	1.2046	1.1999
a (deg)[c]	108.1	123.7	121.9	119.2
energy (hartrees)	−130.298 885	−129.931 145	−114.318 766	−113.925 460

[a] r_H is the NH bond length in HNO and the CH bond length in H_2CO. [b] r_0 is the NO bond length in HNO and the CO bond length in H_2CO. [c] a is the HNO or HCO angle. H_2CO is planar in both the neutral and cation.

TABLE 3: Vibrational Frequencies and Zero-Point Energies[a,b]

	neutral				cation			
HNO	calcd	scale factor	scaled	exptl[c]	calcd	scale factor	scaled	exptl
1 NH stretch	2977.5	0.901	2682.7	2684.0	2939.9	0.901	2648.8	*2648.8*
2 bend	1579.3	0.949	1498.8	1500.8	1078.9	0.981	1058.4	1090[d]
								990[e]
3 NO stretch	1651.9	0.949	1567.7	1565.3	2016.0	0.981	1977.7	1960[d]
								1972[e]
ZPE	3104.4		2874.6	2875.1	3017.4		2914.5	2849.5
ΔZPE[f]								−25.6
ΔZPE (eV)								−0.003

	neutral				cation			
H_2CO	calcd	scale factor	scaled	exptl[g]	calcd	scale factor	scaled	exptl[h]
1 CH_2 sym str	2951.4	0.943	2783.2	2783	2854.5	0.904	2580.5	2580
2 CO str	1816.6	0.964	1751.2	1746	1672.9	0.962	1609.3	1675
3 CH_2 sciss	1556.8	0.964	1500.8	1500	1294.6	0.962	1245.4	1210
4 CH_2 a-str	3016.6	0.943	2844.7	2843	2962.5	0.904	2678.1	*2678*
5 CH_2 rock	1286.8	0.964	1240.5	1249	1096.3	0.962	1054.6	*1055*
6 CH_2 wag	1213.3	0.964	1169.6	1167	877.1	0.962	843.8	777
ZPE	5920.8		5644.9	5644	5379.0		5005.9	4987.5
ΔZPE[f]								−656.5
ΔZPE (eV)								−0.081

[a] All values are in cm^{-1}. [b] The calculated values are at the QCISD/cc-pVTZ level. The scale factors are discussed in the text. The italic numbers in the experimental column are our scaled calculated vibrational frequencies. [c] References 51 and 52. [d] Reference 17b. [e] This work, see text. [f] ZPE(ion) minus ZPE(neutral). [g] Reference 53. [h] References 54 and 55.

TABLE 4: QCISD(T) Calculations on HNO and H_2CO

	HNO		H_2CO	
	neutral	cation	neutral	cation
		Basis Set: cc-pVTZ		
energy (hartrees)	−130.338 641	−129.966 794	−114.369 596	−113.968 959
IE (eV)		10.118		10.902
IE with ΔZPE (eV)		10.115		10.820
IE using reaction 6 (eV)		10.169		
		Basis Set: aug-cc-pVQZ		
energy (hartrees)	−130.343 142	−129.969 347	−114.372 965	−113.971 000
IE (eV)		10.171		10.938
IE with ΔZPE (eV)		10.168		10.856
IE using reaction 6 (eV)		10.186		

TABLE 5: Summary of Thermodynamic Values for HNO

$\Delta_f H°_0$(HNO) (kJ mol^{-1})	IE(HNO) (eV)		$\Delta_f H°_{298}(HNO^+)$ (kJ mol^{-1})	PA_{298}(NO) (kJ mol^{-1})
	vertical	adiabatic		
105.6[29b]	10.66[a]	10.28[a]		
106.2[31c]	10.05[31c]	9.75[31c]	1074[d]	
102.5[22]		10.23 ± 0.14[b]	1071.5[e]	
105 ± 3[23]		10.1 ± 0.1[17a]	1094.9[56,58]	≈531[25]
110.02 ± 0.25[21]	10.56[17b]	10.18 ± 0.01[17b]	1088.8[56,57]	531.4 ± 4.2[61]
		$10.18_4 \pm 0.01_2$[c]	**1089.73 ± 1.18**[c]	**531.55 ± 1.26**[c]

[a] Reference 28 reports a calculated value for the vertical IE of 10.66 eV, which we scale by −0.38 eV (from ref 17b) to obtain 10.28 eV for the adiabatic IE. [b] This value was derived (by Bruna and Marian,[31b] see text) from the EIMS result, 10.29 eV, for $D^{15}NO$ reported by Kohout and Lampe.[14b] [c] This study. [d] McLean et al.[30] report a dissociation energy for HNO^+ (→ H + NO^+) of 147 kJ mol^{-1}, which leads to $\Delta_f H°_0(HNO^+) \approx$ 1077 kJ mol^{-1}, or $\Delta_f H°_{298}(HNO^+) \approx$ 1074 kJ mol^{-1}. [e] This value derived by us from the 0 K result of Kutina et al.[60]

the effect of varying the unknown vibrations on the ZPE, from the difference of the calculated IE for formaldehyde versus the known IE for formaldehyde, and from the change in the calculated IE in going from the cc-pVTZ basis set to the aug-cc-pVQZ basis set.

C. Determination of $\Delta_f H°_T(HNO^+)$ and the Absolute Proton Affinity. By using our value for IE(HNO), $10.18_4 \pm 0.01_2$ eV, and the heat of formation of HNO at zero K, we may readily obtain $\Delta_f H°_0(HNO^+)$

$$\Delta_f H°_0(HNO^+) = IE(HNO) + \Delta_f H°_0(HNO) \qquad (7)$$

For $\Delta_f H°_0$(HNO), we select the value of 110.02 ± 0.25 kJ mol^{-1} derived from the careful bond energy determination of Dixon et al.[21] Thus, we compute $\Delta_f H°_0(HNO^+) = 1092.65 \pm 1.18$ kJ mol^{-1}, where the uncertainty is the root-sum-square of the IE and $\Delta_f H°_0$ uncertainties. By using eq 8

$$\Delta_f H°_{298}(HNO^+) = \Delta_f H°_0(HNO^+) + (H°_{298} - H°_0)_{HNO+} - (H°_{298} - H°_0)_{elements} \qquad (8)$$

together with our *ab initio* calculation of $(H°_{298} - H°_0)_{HNO+} =$ 9.986 kJ mol^{-1} and $(H°_{298} - H°_0)_{elements} =$ 12.909 kJ mol^{-1} (ref 23), we have derived the value $\Delta_f H°_{298}(HNO^+) = 1089.73 \pm 1.18$ kJ mol^{-1}. The value of $\Delta_f H°_{298}(HNO^+)$ obtained here compares well with those determined from an ion−molecule

study.[56] From the proton transfer reaction

$$H_3^+ + NO \rightarrow HNO^+ + H_2 \quad (\Delta_r H = -1.13 \text{ eV})^{56} \quad (9)$$

we compute $\Delta_f H°_{298}(HNO^+) = 1088.8$ kJ mol^{-1} (ref 57), and from the charge transfer reaction

$$HNO^+ + NO \rightarrow NO^+ + HNO \quad (\Delta_r H = -0.98 \text{ eV})^{56} \quad (10)$$

we obtain $\Delta_f H°_{298}(HNO^+) = 1094.9$ kJ mol^{-1} (ref 58). In contrast, there is poor agreement between the present result for $\Delta_f H°_{298}(HNO^+)$ and that of Kutina et al.,[59] who report a value of 1074.4 kJ mol^{-1} at 0 K (or, we compute, 1071.5 kJ mol^{-1} at 298 K). The value for $\Delta_f H°_0(HNO^+)$ reported by Kutina et al.[59] was determined from a very weak and indistinct threshold for dissociative ionization of NH_2OH at 11.51 eV with a stated uncertainty of ±0.06 eV. Since the process leading to HNO^+-$(+H_2)$ is the lowest energy dissociation channel, it is somewhat surprising that their derived enthalpy differs from the present value by such a large amount (≈18 kJ mol^{-1}). By using a recently evaluated quantity (−50 ± 10 kJ mol^{-1}) for $\Delta_f H°_0(NH_2$-$OH)$,[23] we can account for about 1 kJ mol^{-1} of the discrepancy. The remaining difference, ≈17 (± 12) kJ mol^{-1}, would correspond to a larger appearance energy (AE) than was reported by Kutina et al.[59] (≈11.69 eV instead of the reported value of 11.51 eV), and, indeed, this larger AE value appears to be consistent with the spectrum presented in ref 59. Nevertheless, the difference noted here, while not highly significant, might reflect errors either in the AE measurement or in the value for $\Delta_f H°_0(NH_2OH)$ or possibly in both.

Finally, by using our derived value for $\Delta_f H°_0(HNO^+)$ and known values for $\Delta_f H°_0$ of NO and H^+, we can determine the absolute proton affinity of NO at 0 K.

$$PA(NO) = \Delta_f H°(NO) + \Delta_f H°(H^+) - \Delta_f H°(HNO^+) \quad (11)$$

From $\Delta_f H°_0(HNO^+) = 1092.65 \pm 1.18$ kJ mol^{-1}, the standard value for $\Delta_f H°_0(NO) = 90.773 \pm 0.43$ kJ mol^{-1} (ref 23), and $\Delta_f H°_0(H^+) = 1528.0$ kJ mol^{-1} (ref 26), PA(NO) is readily evaluated by using eq 11 to obtain $PA_0(NO) = 526.12 \pm 1.26$ kJ mol^{-1}. Similarly, a value for the proton affinity of NO at 298 K may be derived from $\Delta_f H°_{298}(HNO^+) = 1089.73 \pm 1.18$ kJ mol^{-1} (see above), the standard value for $\Delta_f H°_{298}(NO) = 91.277 \pm 0.43$ kJ mol^{-1} (ref 23), and $\Delta_f H°_{298}(H^+) = 1530.0$ kJ mol^{-1} (ref 26), to obtain $PA_{298}(NO) = 531.55 \pm 1.26$ kJ mol^{-1}. This value of the absolute $PA_{298}(NO)$ is in excellent agreement with the evaluated value of ∼531 kJ mol^{-1} from Lias et al.[25] and with the value of 531.4 ± 4.2 kJ mol^{-1} that was deduced by Adams et al.[60] from a measurement of the proton affinity difference between NO and CF_4.

In conclusion, we have determined values for IE(HNO) *via* photoionization mass spectrometry ($10.18_4 \pm 0.01_2$ eV) and by using *ab initio* molecular orbital calculations (10.186 ± 0.050 eV). These results are listed in Table 5 along with other thermodynamic data for HNO. The agreement between the present results and that of an earlier PES study (10.18 ± 0.01 eV)[17b] is excellent, and thus the accuracy of the three determinations is compelling. In addition, we have computed values for $\Delta_f H°_{298}(HNO^+)$ and $PA_{298}(NO)$ that agree very well with those obtained by completely different methods.[56,60] This level of agreement demonstrates a high degree of internal consistency in the values employed in the various thermodynamic cycles.

Acknowledgment. The work at BNL was supported by the Chemical Sciences Division, Office of Basic Energy Sciences, U.S. Department of Energy, under Contract No. DE-AC02-76CH00016. The work at GSFC was supported by the NASA Planetary Atmospheres Research Program. Z.Z. was supported under the Laboratory Directed Research and Development Program at Brookhaven National Laboratory. P.S.M. and R.P.T. thank the NAS/NRC for the award of Research Associateships.

References and Notes

(1) Baulch, D. L.; Drysdale, D. D.; Horne, D. G. *Evaluated Kinetic Data for High Temperature Reactions*; Butterworths: London, 1973; Vol. 2.

(2) (a) Hanson, R. K.; Salimian, S. In *Combustion Chemistry*; Gardiner, W. G., Jr., Ed.; Springer-Verlag: New York, 1984 and references therein. (b) Tsang, W.; Herron, J. T. *J. Phys. Chem. Ref. Data* **1991**, *20*, 609.

(3) (a) Ulich, B. L.; Hollis, J. M.; Snyder, L. E. *Astrophys. J. Lett.* **1977**, *217*, L105. (b) Snyder, L. E.; Kuan, Y. J.; Ziurys, L. M.; Hollis, J. M. *Astrophys. J. Lett.* **1993**, *403*, L17.

(4) Herbst, E. *Annu. Rev. Phys. Chem.* **1995**, *46*, 27.

(5) Smallwood, H. M. *J. Am. Chem. Soc.* **1929**, *51*, 1985.

(6) (a) Clyne, M. A. A.; Thrush, B. A. *Trans. Faraday Soc.* **1961**, *57*, 1305. (b) Clyne, M. A. A.; Thrush, B. A. *Discuss. Faraday Soc.* **1962**, *33*, 139.

(7) (a) Sugden, T. M.; Bulewicz, E. M.; Demerdache, A. *Chemical Reactions in the Lower and Upper Atmosphere*; Interscience: New York, 1961; p 89. (b) Bulewicz, E. M.; Sugden, T. M. *Proc. R. Soc. London A.* **1964**, *277*, 143.

(8) Halstead, C. J.; Jenkins, D. R. *Chem. Phys. Lett.* **1968**, *2*, 281.

(9) (a) Miller, J. A.; Branch, M. C.; Kee, R. J. *Combust. Flame* **1981**, *43*, 81 and references therein. (b) Miller, J. A. *Combust. Res. Bull. No. 5*; Sandia National Laboratories: Livermore, CA, July, 1981.

(10) Natarajan, K.; Mick, H. J.; Woiki, D.; Roth, P. *Combust. Flame* **1994**, *99*, 610.

(11) (a) Diau, E. W.; Halbgewachs, M. J.; Smith, A. R.; Lin, M. C. *Int. J. Chem. Kinet.* **1995**, *27*, 867. (b) Mebel, A. M.; Morokuma, K.; Lin, M. C.; Melins, C. F. *J. Phys. Chem.* **1995**, *99*, 1900. (c) Mebel, A. M.; Lin, M. C.; Morokuma, K.; Melius, C. F. *Int. J. Chem. Kinet.* **1996**, *28*, 693.

(12) Harteck, P. *Ber. Dtsch. Chem. Ges.* **1933**, *66*, 423.

(13) Dalby, F. W. *Can. J. Phys.* **1958**, *36*, 1336.

(14) (a) Kohout, F. C.; Lampe, F. W. *J. Am. Chem. Soc.* **1965**, *87*, 5795. (b) Kohout, F. C.; Lampe, F. W. *J. Chem. Phys.* **1966**, *45*, 1074.

(15) Lambert, R. M. *Chem. Commun.* **1966**, 850.

(16) Seel, F.; Bliefert, C. *Z. Anorg. Allg. Chem.* **1974**, *406*, 277.

(17) (a) Fehér, M. Ph.D. Thesis, University of Southhampton, 1987, as quoted in ref 17b. (b) Baker, J.; Butcher, V.; Dyke, J. M.; Morris, A. *J. Chem. Soc., Faraday Trans.* **1990**, *86*, 3843.

(18) (a) Clement, M. J. Y.; Ramsay, D. A. *Can. J. Phys.* **1961**, *39*, 205. (b) Bancroft, J. L.; Hossas, J. M.; Ramsay, D. A. *Can. J. Phys.* **1962**, *40*, 322. (c) Ramsay, D. A.; Zhu, Q.-S. *J. Chem. Soc., Faraday Trans.* **1995**, *91*, 2975.

(19) Callear, A. B.; Wood, P. M. *Trans. Faraday Soc.* **1971**, *67*, 3399.

(20) Clough, P. N.; Thrush, B. A.; Ramsay, D. A.; Stamper, J. G. *Chem. Phys. Lett.* **1973**, *23*, 155.

(21) (a) Dixon, R. N.; Jones, K. B.; Noble, M.; Carter, S. *Mol. Phys.* **1981**, *42*, 455. (b) Dixon, R. N. *J. Chem. Phys.* **1996**, *104*, 6905.

(22) Chase, M. W., Jr.; Davies, C. A.; Downey, J. R., Jr.; Frurip, D. J.; McDonald, R. A.; Syverud, A. N. *J. Phys. Chem. Ref. Data, Suppl. 1* **1985**, *14*.

(23) Gurvich, L. V.; Veyts, I. V.; Alcock, C. B. *Thermodynamic Properties of Individual Substances*, 4th ed.; Hemisphere Publishing Corp.; New York, 1991; Vol. 1.

(24) Levin, R. D.; Lias, S. G. *Ionization Potential and Appearance Potential Measurements, 1971−1981*; National Standards Reference Data Series 71; National Bureau of Standards: Gaithersburg, MD, 1982.

(25) Lias, S. G.; Liebman, J. F.; Levin, R. D. *J. Phys. Chem. Ref. Data* **1984**, *13*, 695.

(26) Lias, S. G.; Bartmess, J. E.; Liebman, J. F.; Holmes, J. L.; Levin, R. D.; Mallard, W. G. *J. Phys. Chem. Ref. Data Suppl. 1* **1988**, *17*.

(27) Lias, S. G.; Liebman, J. F.; Levin, R. D.; Kafafi, S. A. *Positive Ion Energetics Version 2.0*; NIST Standard Reference Database 19A; NIST: Gaithersburg, MD, 1993.

(28) Chong, D. P.; Herring, F. G.; McWilliams, D. *J. Electron Spectrosc. Relat. Phenom.* **1975**, *7*, 445.

(29) (a) Seeger, R.; Pople, J. A. *J. Chem. Phys.* **1976**, *65*, 265. (b) Curtiss, L. A.; Raghavachari, K.; Trucks, G. W.; Pople, J. A. *J. Chem. Phys.* **1991**, *94*, 7221.

(30) McLean, A. D.; Loew, G. H.; Berkowitz, D. S. *Mol. Phys.* **1978**, *36*, 1359.

(31) (a) Bruna, P. J.; Marian, C. M. *Chem. Phys. Lett.* **1979**, *67*, 109. (b) Bruna, P. J.; Marian, C. M. *Chem. Phys.* **1979**, *37*, 425. (c) Bruna, P. J. *Chem. Phys.* **1980**, *49*, 39.

(32) (a) Walch, S. P.; Rohlfing, C. M. *J. Chem. Phys.* **1989**, *91*, 2939. (b) Guadagnini, R.; Schatz, G. C.; Walch, S. P. *J. Chem. Phys.* **1995**, *102*, 784.

(33) (a) Lee, T. J. *J. Chem. Phys.* **1993**, *99*, 9783. (b) Lee, T. J. *Chem. Phys. Lett.* **1994**, *223*, 431. (c) Dateo, C. E.; Lee, T. J.; Schwenke, D. W. *J. Chem. Phys.* **1994**, *101*, 5853. (d) Lee, T. J.; Dateo, C. E. *J. Chem. Phys.* **1995**, *103*, 9110.

(34) Sengupta, D.; Chandra, A. K. *J. Chem. Phys.* **1994**, *101*, 3906.

(35) Nesbitt, F. L.; Marston, G.; Stief, L. J.; Wickramaaratchi, M. A.; Tao, W.; Klemm, R. B. *J. Phys. Chem.* **1991**, *95*, 7613.

(36) Tao, W.; Klemm, R. B.; Nesbitt, F. L.; Stief, L. J. *J. Phys. Chem.* **1992**, *96*, 104.

(37) Monks, P. S.; Stief, L. J.; Krauss, M.; Kuo, S.-C.; Klemm, R. B. *Chem. Phys. Lett.* **1993**, *211*, 416.

(38) Kuo, S.-C.; Zhang, Z.; Klemm, R. B.; Liebman, J. F.; Stief, L. J.; Nesbitt, F. L. *J. Phys. Chem.* **1994**, *98*, 4026.

(39) Buckley, T. J.; Johnson, R. D., III; Huie, R. E.; Zhang, Z.; Kuo, S.-C.; Klemm, R. B. *J. Phys. Chem.* **1995**, *99*, 4879.

(40) Grover, J. R.; Walters, E. A.; Newman, J. K.; White, M. C. *J. Am. Chem. Soc.* **1985**, *107*, 7329 and references therein.

(41) DeMore, W. B.; Sander, S. P.; Golden, D. M.; Hampson, R. F.; Kurylo, M. J.; Howard, C. J.; Ravishankara, A. R.; Kolb, C. E.; Molina, M. J. *Chemical Kinetics and Photochemical Data for Use in Stratospheric Modeling, Evaluation Number 11*; JPL Publication 94-26; JPL: Pasadena, CA, 1994.

(42) Tsang, W.; Hampson, R. F. *J. Phys. Chem. Ref. Data* **1986**, *15*, 1087.

(43) Tsang, W.; Herron, J. T. *J. Phys. Chem. Ref. Data* **1991**, *20*, 609.

(44) *CRC Handbook of Chemistry and Physics*, 68th ed.; Weast, R. C., Ed.; CRC Press, Inc.: Boca Raton, FL, 1987.

(45) Kee, R. J.; Rupley, F. M.; Miller, J. A. *CHEMKIN-II: A Fortran Chemical Kinetic Package for the Analysis of Gas-Phase Chemical Kinetics*; Sandia National Laboratories Report SAND89-8009; Sandia National Laboratories; Livermore, CA, 1989.

(46) Frisch, M. J.; Trucks, G. W.; Schlegel, H. B.; Gill, P. M. W.; Johnson, B. G.; Robb, M. A.; Cheeseman, J. R.; Keith, T.; Petersson, G. A.; Montgomery, J. A.; Raghavachari, K.; Al-Laham, M. A.; Zakrzewski, V. G.; Ortiz, J. V.; Foresman, J. B.; Cioslowski, J.; Stefanov, B. B.; Nanayakkara, A.; Challacombe, M.; Peng, C. Y.; Ayala, P. Y.; Chen, W.; Wong, M. W.; Andres, J. L.; Replogle, E. S.; Gomperts, R.; Martin, R. L.; Fox, D. J.; Binkley, J. S.; Defrees, D. J.; Baker, J.; Stewart, J. P.; Head-Gordon, M.; Gonzalez, C.; Pople, J. A. *Gaussian 94, Revision A.1*; Gaussian, Inc.: Pittsburgh, PA, 1995.

(47) Drury-Lessard, C. R.; Moule, D. C. *Chem. Phys. Lett.* **1977**, *47*, 300.

(48) Guadagnini, R.; Schatz, G. C.; Walch, S. P. *J. Chem. Phys.* **1995**, *102*, 774.

(49) Robins, K. A.; Farley, J. W.; Toto, J. L. *J. Chem. Phys.* **1993**, *99*, 9770.

(50) Heiberg, A.; Almlöf, J. *Chem. Phys.* **1982**, *85*, 542.

(51) Petersen, J. C.; Vervloet, M. *Chem. Phys. Lett.* **1987**, *141*, 499.

(52) Johns, J. W. C.; McKellar, A. R. W. *J. Chem. Phys.* **1977**, *66*, 1217.

(53) Shimanouchi, T. *Tables of Molecular Vibrational Frequencies. Consolidated Volume 1*; NSRDS-NBS-39; National Bureau of Standards: Washington, DC, 1992.

(54) Baker, A. D.; Baker, C.; Brundle, C. R.; Turner, D. W. *Int. J. Mass Spectrom. Ion Phys.* **1968**, *1*, 285.

(55) (a) Niu, B.; Shirley, D. A.; Bai, Y.; Daymo, E. *Chem. Phys. Lett.* **1993**, *201*, 212. (b) Niu, B.; Shirley, D. A.; Bai, Y. *J. Chem. Phys.* **1993**, *98*, 4377.

(56) Burt, J. A.; Dunn, J. L.; McEwan, M. J.; Sutton, M. M.; Roche, A. E.; Schiff, H. I. *J. Chem. Phys.* **1970**, *52*, 6062.

(57) For reaction 9: $\Delta_f H°_{298}(H_3^+) = 1106.6$ kJ mol^{-1} (ref 26); $\Delta_f H°_{298}(NO) = 91.277$ kJ mol^{-1} (ref 23); $\Delta_f H°_{298}(H_2) = 0$ kJ mol^{-1}; $\Delta_r H = -109.03$ kJ mol^{-1}. Thus, $\Delta_f H°_{298}(HNO^+) = 1106.6 + 91.277 - 0 - 109.03 = 1088.8$ kJ mol^{-1}.

(58) For reaction 10: $\Delta_f H°_{298}(NO) = 91.277$ kJ mol^{-1} (ref 23); $\Delta_f H°_{298}(HNO) = 107.05$ kJ mol^{-1} (ref 21); $\Delta_f H°_{298}(NO^+) = 984.61$ kJ mol^{-1} (ref 26); $\Delta_r H = -94.56$ kJ mol^{-1}. Thus, $\Delta_f H°_{298}(HNO^+) = 107.05 + 984.61 - 91.277 + 94.56 = 1094.9$ kJ mol^{-1}.

(59) Kutina, R. E.; Goodman, G. L.; Berkowitz, J. *J. Chem. Phys.* **1982**, *77*, 1664.

(60) Adams, N. G.; Smith, D.; Tichy, M.; Javahery, G.; Twiddy, N. D. *J. Chem. Phys.* **1989**, *91*, 4037.